Separation and Purification Technology 292 (2022) 120944

Contents lists available at ScienceDirect

Separation and Purification Technology

journal homepage: www.elsevier.com/locate/seppur

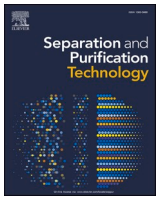

# Strategies to increase ion selectivity in electrodialysis

T.M. Mubita [a,b], S. Porada [b], P.M. Biesheuvel [b], A. van der Wal [a,c], J.E. Dykstra [a,*]

[a] Environmental Technology, Wageningen University, Bornse Weilanden 9, 6708 WG Wageningen, the Netherlands
[b] Wetsus, European Centre of Excellence for Sustainable Water Technology, Oostergoweg 9, 8911 MA Leeuwarden, the Netherlands
[c] Evides Water Company, Schaardijk 150, 3063 NH Rotterdam, the Netherlands

ARTICLE INFO

*Keywords:*
Electrodialysis
Nernst-Planck equation
Ion-exchange membranes
Ion selectivity

ABSTRACT

We analyze selective removal of anions in electrodialysis (ED) from a multicomponent ion mixture where all ions are monovalent, both experimentally, and by a modified theory. The theory makes use of the Nernst-Planck equation to describe transport of ions across ion-exchange membranes in combination with the ion affinity, which is a parameter that accounts for the preference of membrane materials to adsorb one ion more than another. For a mixture of $NO_3^-$ and $Cl^-$ anions, ion affinity was measured in an adsorption experiment, and it was found that $NO_3^-$ adsorbs more in anion-exchange membranes (AEMs) than $Cl^-$. Faster transport of $NO_3^-$ relative to $Cl^-$ in batch-mode ED experiments is well described by the transport theory, for three types of AEMs that we tested. From analysis of the model, we can derive that membrane selectivity in ED between different anions can be increased further by: i) an increase in the difference in ion affinity of the anions, ii) an increase in the AEM thickness, and iii) a decrease in the charge density of the AEM. The last two strategies go against the general understanding that thin highly charged membranes are in general better for ED. Our proposed strategies follow rigorously from our combined theoretical–experimental study.

## 1. Introduction

Ion-exchange membranes (IEMs) are the key components of technologies such as electrodialysis (ED) and membrane capacitive deionization (MCDI), which separate ions from saline streams [3,14,22,33]. In the present study, we focus on ion separation using ED. The main application of ED technology is the removal of a large part of the salt ions from a water stream. However, there are specific applications of ED where separation between ions of the same charge sign but with different valency is required, e.g., separation of $Na^+$-ions from $Ca^{2+}$-ions in water softening, or separation of ions with the same valency, for instance the separation of $NO_3^-$-ions from groundwater, which also contain $Cl^-$-ions.

In ED, the potential to selectively separate ions of the same charge sign is mostly determined by the structure of the IEMs, such as the density of ion-exchange sites, the pore structure of the membrane matrix, and by properties of the ions, such as their hydrated size and hydration energy [4,5,15,16,17,26]. Additionally, operational conditions, such as applied current and volumetric flow rate, and the composition of the solution to be treated, affect ion separation [11,25,30].

Experimental and theoretical studies report on the measurement of ion selectivity in IEMs and the mechanisms underlying ion transport through IEMs [6,18,20,21]. Theoretical models often use the Nernst–-Planck equation which describes that ion transport is due to diffusional and migrational forces. These transport models include membrane characteristics, such as porosity, charge density, ion partitioning at the membrane-solution interface, and ion diffusion coefficients [19,28,29].

Also transport in multicomponent solutions has been discussed in the literature. Competitive transport between mono- and divalent ions is often described by considering ion transport in the diffusion boundary layer adjacent to the IEM, and the influence of the applied current density [13,32]. Kim et al. [13] reported that at low current density the divalent ions are preferentially transported, whereas at high current density concentration polarization favors the transport of monovalent ions. Galama et al. [7] studied the influence of divalent ions present in seawater on the electrochemical properties of anion exchange membranes (AEMs) and cation-exchange membranes (CEMs) under low current conditions. This study presented a transport theory that describes ion selectivity as the result of the differences in diffusion coefficients between mono- and divalent ions inside the membrane.

Interestingly, only a few studies theoretically describe preferential transport of ions with equal valence in ED [9,31]. Just like we will do,

* Corresponding author.
*E-mail address:* jouke.dykstra@wur.nl (J.E. Dykstra).

https://doi.org/10.1016/j.seppur.2022.120944
Received 19 January 2022; Received in revised form 9 March 2022; Accepted 26 March 2022
Available online 30 March 2022
1383-5866/© 2022 The Authors. Published by Elsevier B.V. This is an open access article under the CC BY license (http://creativecommons.org/licenses/by/4.0/).

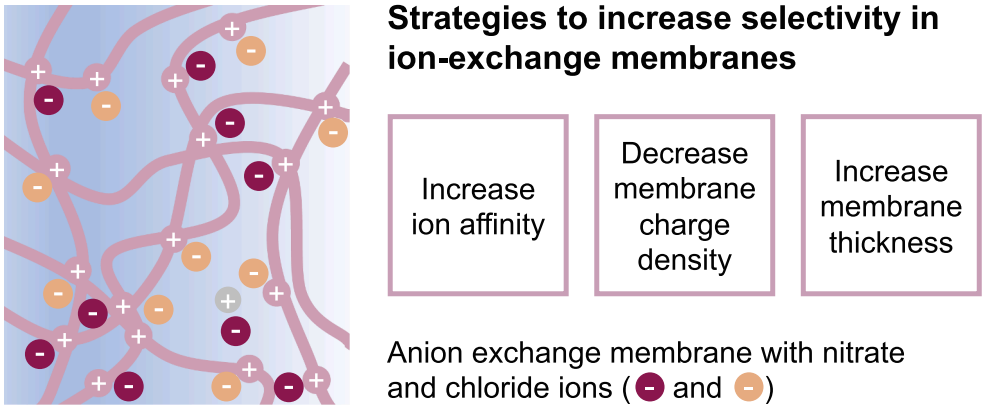


**Fig. 1.** Schematic of possible strategies to increase nitrate selectivity in ion-exchange membranes.

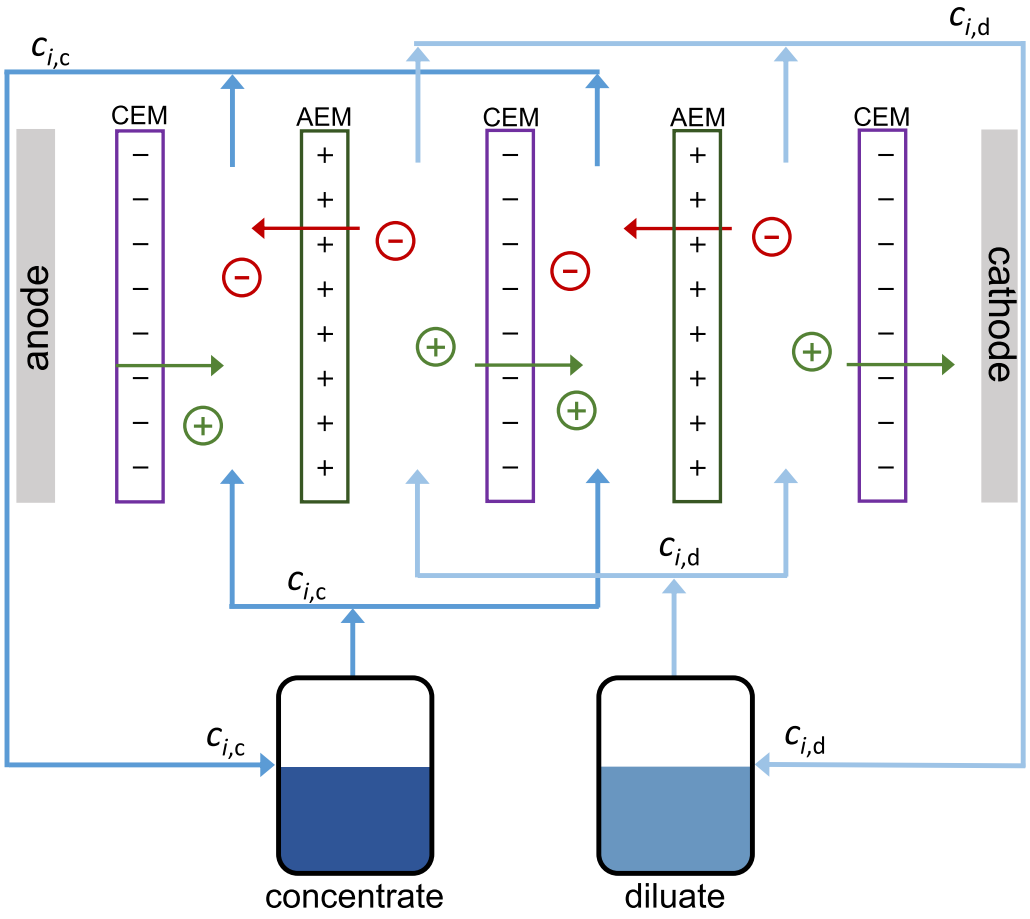


**Fig. 2.** A schematic representation of an electrodialysis system operated in batch-mode.

these transport models also use the Boltzmann equation to describe the equilibrium distribution of ions on the solution–membrane interfaces, and modify it by including a difference in hydration energies between the ions, and that hydration energy is a function of ion size. Using this approach, for instance, Yang and Pintauro [31] described the preferential adsorption and transport of alkali-metal cations in multicomponent solutions in a dialysis experiment (i.e., without an applied current).

In the present work, we present theory to describe the transport of mixtures of monovalent ions through IEMs in ED. In the theory for electrochemical equilibrium at the membrane-solution interfaces, we account for differences in the affinity of the membrane towards different types of ions. We use this approach to predict the transport of $Cl^-$- and $NO_3^-$-ions across different IEMs, which are two commercial membranes (homogeneous and heterogeneous) and a home-made heterogeneous AEM. In a previous study, we reported the fabrication and characterization of these AEMs, which showed an increased selectivity towards $NO_3^-$ over $Cl^-$ [15]. This study evaluated the effect of alkyl length substituents in quaternary ammonium groups on membrane properties, such as water content. Increased $NO_3^-$ selectivity was attributed to a decrease in water content, and therefore to an increase in membrane hydrophobicity, with increasing alkyl chain length. The combined effects of higher hydrophobicity and an increase in steric hindrance due to larger alkyl groups, likely lead to partial loss of water molecules in the hydration shells of the counterions. Ions with lower hydration energies,

**Table 1**
Properties of the membranes used in the present study.

| | Charge density * $X$ (M) | Thickness $\delta_m$ (μm) | $NO_3^-$-membrane affinity, $\mu_{NO_3^-}$ |
|---|---|---|---|
| **AEM** | | | |
| Newly-designed AEM | 4.52 | 135 | 1.83 |
| Neosepta, AMX | 7.56 | 150 | 1.35 |
| Ralex, AMH-PES | 4.75 | 590 | 0.77 |
| **CEM** | | | |
| Neosepta, CMX | 8.70 | 150 | – |
| Ralex, CMH-PES | 5.75 | 590 | – |

* The charge density is calculated based on the measured water content and ion exchange capacity reported in Mubita et al. [15].

in this case $NO_3^-$, dehydrate more easily and are transported preferentially across the membranes [6,24,26,27].

The present study builds on our previous work [15] and focuses on understanding the selectivity between $NO_3^-$ and $Cl^-$ due to different transport rates across an AEM in ED. We present experimental results for equilibrium adsorption and transport in a small ED stack, and compare both sets of experiments (for three types of membranes) with theoretical predictions. In addition, we analyze results of theoretical calculations to develop strategies for enhanced selectivity (Fig. 1) by changing membrane properties such as ion affinity, membrane thickness, and membrane charge density.

## 2. Theory

In this section we describe theory for the transport of ions in an ED system in case of a mixture containing more than two types of ions (multicomponent solution). The ED system is operated in batch-mode and consists of i) the ED stack with multiple cell pairs, each of which includes one AEM, one CEM, and the diluate and concentrate spacer channels, and ii) two reservoirs with the diluate and concentrate solutions. These solutions are kept separate from one another and are continuously recirculated between the reservoirs and the ED stack (Fig. 2).

We first describe the ionic flux, $J_i$, (unit mol/m$^2$/s) through non-ideal IEMs, i.e., membranes through which not only counterions are transported, but co-ions as well. We assume that diffusion and electromigration only take place in the direction perpendicular to the membrane surface ($x$-direction), and we neglect water transport through the IEMs. Thus, we use a simplification of the Nernst-Planck equation without convective transport, given by [1,34]

$$J_i = -D_{m,i}\left(\frac{\partial c_{m,i}}{\partial x} + z_i c_{m,i}\frac{\partial \phi}{\partial x}\right) \tag{1}$$

where subscript $i$ refers to the ion type, $c_{m,i}$ is ion concentration per volume of solution in the membrane (mol/m$^3$), $x$ the position inside the membrane, $z_i$ ion valence, $\phi$ the dimensionless electrical potential ($\phi = \frac{V}{V_T}$, where $V_T$ is thermal voltage, with $V_T = \frac{RT}{F} \sim 25.7$ mV), and $D_{m,i}$ is the ion diffusion coefficient in the membrane (m$^2$/s), which is lower than the ion diffusion coefficient in free solution, i.e., $D_{m,i} = D_{\infty,i}/f_{red,i}$. For the anions in the AEM, the reduction factor, $f_{red,i}$, is empirically obtained from fitting the model to data, whereas for all ions in the CEM, this factor was set to 10 [29], see Table 1. We include in the theory that the values of $D_{\infty,i}$, and thus of $D_{m,i}$, are different for each ion.

Assuming locally steady-state, at each position in the membrane, mass conservation of ions is given by

$$\frac{\partial J_i}{\partial x} = 0 \tag{2}$$

which is evaluated for each type of ion together with the electroneutrality condition, which holds at each position in the membrane as well,

$$\sum_i z_i c_{m,i} + \omega X = 0 \tag{3}$$

where ω is the sign of the membrane charge, i.e., ω =+1 for the AEM and ω = -1 for the CEM, and $X$ is the charge density of the membrane, defined in moles of charges per unit volume of solution phase in the membrane.

We also evaluate the current density, $I$ (A/m$^2$), which is independent of $x$, i.e., it has the same value at each position in the membranes and in the spacer channels, and is given by

$$I = F \bullet \sum_i z_i J_i \tag{4}$$

where $F$ is Faraday's constant (96485 C/mol).

The ion concentration inside the membrane at the interface with a spacer channel, $c_i^*$, is often described by the Boltzmann equation [8,23,29]. We include an ion affinity term, μ, which describes that an IEM can preferentially adsorb one ion over another from multi-ionic solutions. The ion affinity term combines all possible contributions (chemical and physical), such as size-based interactions, but does not include the electrostatic Donnan effect. Thus, the ion concentration inside the membrane at each of the solution/membrane interfaces is given by

$$c_i^* = c_{i,j} \bullet \exp\left(-z_i \bullet \Delta\phi_{D,j} + \mu_i\right) \tag{5}$$

where index $j$ refers to either the concentrate or diluate spacer channel, and $\Delta\phi_{D,j}$ is the Donnan potential at that interface. In case of a high fixed membrane charge density, $X$, then this membrane charge is predominantly compensated by counterions (such as anions in an AEM), and then only the difference between the μ-values of the two or more counterions is of importance, not their absolute values. Therefore, we can arbitrarily set $\mu_{Cl^-} = 0$ in this paper, and use a non-zero value of $\mu_{NO_3^-}$, because only the difference between the two μ-factors is of importance.

Next, we set up expressions for the ion concentration in the spacer channels, $c_{i,j}$. In the spacer channels, we assume ideally-stirred solutions, and thus we assume the ion concentration is invariant in the $x$-direction (from membrane to membrane) as well as in the direction along the membrane. This assumption is valid in the present work, because the ion removal per pass is only around 1 mM (from a solution with concentrations initially 50 mM) and the residence time for water and ions in a channel is very short, only a few seconds. Because of the low removal per pass, we assume that we can neglect concentration profiles both in $x$- and $y$-direction in the ED channels [2]. In future work the accuracy of this assumption must be further assessed. In real-life applications, with ongoing desalination in the $y$-direction, through the cell, we can expect that concentration polarization is of importance (concentration profiles in direction towards the membranes), and a more detailed ED model will be necessary [2].

Because of the high circulation rate through the ED stack, with a residence time there of only a few seconds, we can combine all separate volumes on the diluate side (stack, tubings, reservoir) into one overall balance, and the same assumption can be used for all volumes on the concentrate side. Such an overall balance for one of the ions is

$$V_j \frac{\partial c_{i,j}}{\partial t} = \pm A\left(J_{i,AEM} - J_{i,CEM}\right) \tag{6}$$

where $V_j$ is either the total diluate volume, or the total concentrate volume, and the $J_{i,k}$'s are the ionic fluxes across the AEM and CEM, and with $A$ the area of all AEMs in the stack which is also the area of all CEMs. The sign of the fluxes, ±, depends on which channel is considered. The electroneutrality condition, Eq. (3), also holds in each solution volume (in that case, $X = 0$ is implemented in Eq. (3)).

**Table 2**
Parameters used in the ED model to describe ion selectivity in IEMs.

| | | | |
|---|---|---|---|
| **Operational** | | | |
| $I$ | Current density | 20 | A/m$^2$ |
| $\Phi_d$, $\Phi_c$ | Flow rate through the diluate/concentrate channels | 20 | mL/min |
| | Number of cell pairs | 4 | |
| $V$ | Volume of reservoir, stack and tubing for: | | |
| | Diluate | 76 | mL |
| | Concentrate | 73 | mL |
| **Spacer channel (diluate and concentrate)** | | | |
| $\delta_{sc}$ | Spacer channel thickness | 450 | μm |
| | Membrane area | 6 | cm$^2$ |
| **Anion Exchange Membranes** | | | |
| $f_{red,i}$ | Reduction factor for ion diffusion coefficient in AEM | | |
| | $K^+$ | 140 | |
| | $Cl^-$ | 140 | |
| | $NO_3^-$ | 115 | |
| **Cation Exchange Membranes** | | | |
| $f_{red,i}$ | Reduction factor for ion diffusion coefficient in CEM | 10 | |
| **Diffusion coefficient of ions in free solution, $D_{\infty,i}/D_{ref}$ ($D_{ref} = 10^{-9}$ m$^2$/s)** | | | |
| | $K^+$ | 1.96 | m$^2$/s |
| | $Cl^-$ | 2.03 | m$^2$/s |
| | $NO_3^-$ | 1.90 | m$^2$/s |

The preferential transport of anions (of ion type $a$ over type $b$) across an AEM is quantified by a time-dependent separation factor, $\beta_{a/b}$, given by

$$\beta_{a/b} = \left(\frac{J_{a,AEM}}{J_{b,AEM}}\right)_t \bullet \left(\frac{c_{b,d}}{c_{a,d}}\right)_t . \quad (7)$$

The above equations (Eq. (1)–Eq. (7)) result in a model that can be solved for an ED system containing a mixture of ions of any valency. We use these equations to describe the selective transport of monovalent ions through three different AEMs, i.e., two commercial AEMs (one homogeneous and one heterogeneous), and a newly-designed heterogeneous AEM [15]. Table 1 and 2 summarize the parameters used in the model for a system of the cation $K^+$ and anions $Cl^-$ and $NO_3^-$ and also provide key information of the ion-exchange membranes.

## 3. Experimental

Adsorption experiments (Section 3.1) were carried out as well as ED experiments (Section 3.2), in all cases with three different anion exchange membranes (AEMs): i) the commercial homogeneous membrane Neosepta AMX (ASTOM Corporation, Tokyo, Japan), ii) the commercial heterogeneous membrane Ralex AMH-PES (Mega a.s., Czech Republic), and iii) a newly-designed heterogeneous membrane. The fabrication and characterization of this membrane is described by Mubita et al. [15].

### 3.1. Adsorption equilibrium experiments

To determine the ion affinity of the IEMs for $NO_3^-$, $\mu_{NO_3^-}$, vs. that for $Cl^-$, we measured the concentration of anions in IEMs in an adsorption experiment. First, membrane pieces of 12 cm$^2$ were immersed for 24 h in 100 mL of aqueous solution (solution A) containing salt mixtures with different concentration ratios of $Cl^-$ to $NO_3^-$ (initial total ionic strength, before immersion, was always 100 mM). Then, the membranes were immersed for a short time, around 2 s, in deionized water to remove the salt solution from the membrane surface. Subsequently, the membranes were transferred into an exchange solution (100 mL, 0.25 M $Na_2SO_4$) for 24 h. After this period, the ion concentrations in the exchange solution were measured by ion chromatography. To ensure a complete release of $Cl^-$ and $NO_3^-$, the membranes were once more placed in a smaller volume of fresh exchange solution for 24 h. The $Cl^-$ and $NO_3^-$ concentrations in the second exchange solution were below the detection limit, implying that we can assume that all $Cl^-$ and $NO_3^-$ ions were released into the first exchange solution. The $NO_3^-$ to $Cl^-$ adsorption selectivity, $S$, of the IEMs was calculated by

$$S_{NO_3^-/Cl^-} = \left(\frac{c_{NO_3^-}}{c_{Cl^-}}\right)_{exchange\ solution} \cdot \left(\frac{c_{Cl^-}}{c_{NO_3^-}}\right)_{solutionA,after24h} . \quad (8)$$

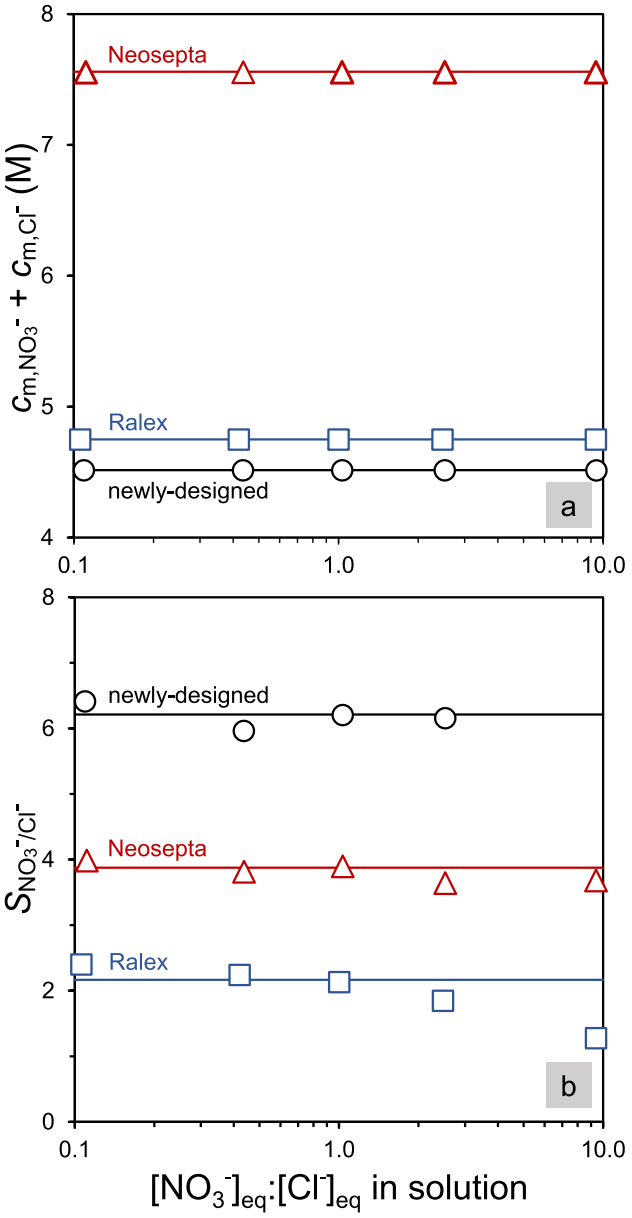


**Fig. 3.** Experimental results (symbols) of adsorption experiments. The membranes were immersed in electrolyte solutions with different $NO_3^-$ and $Cl^-$ concentrations (total ionic strength 100 mM). The $x$-axis gives the equilibrium (eq) $NO_3^-$:$Cl^-$ concentration ratio in solution. a) Total anion concentration in the AEMs ($c_{m,NO_3^-} + c_{m,Cl^-}$). Lines represent the charge density measured in the membranes ,$X$, as reported in Table 1; b) Nitrate selectivity ($S_{NO_3^-/Cl^-}$, Eq. (10)) in the AEMs as function of the ion concentration ratio in the bulk solution. Lines result from fitting theory to the experimental data.

### 3.2. Electrodialysis experiments

The ED experiments were conducted using a micro-ED stack (ED 08002, PCCell GmbH, Germany) consisting of two electrode compartments, one with a Pt/Ir coated titanium anode and the other with a stainless-steel cathode, and four cell pairs. Each cell pair consists of a CEM, a diluate channel, an AEM, and a concentrate channel. The IEMs

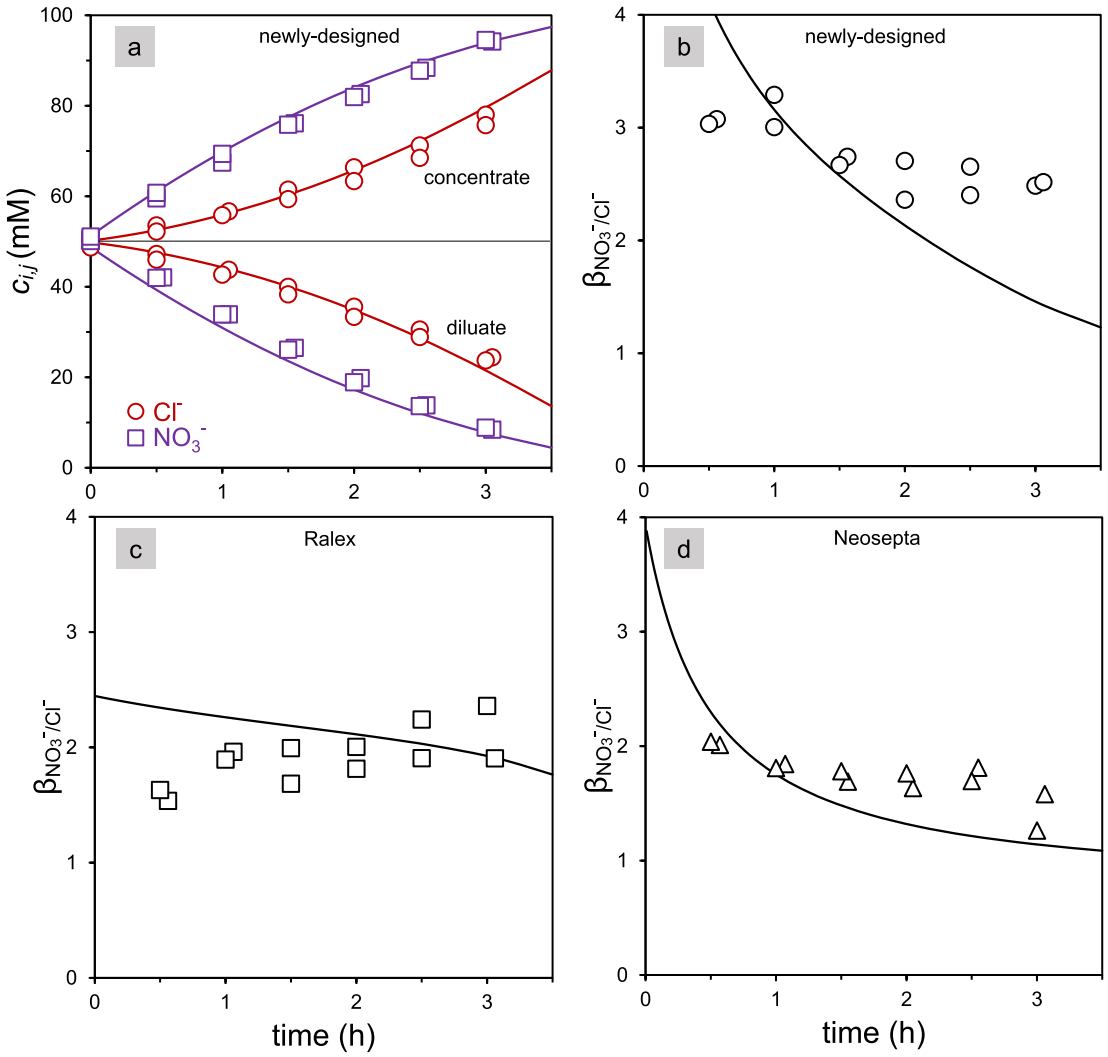


**Fig. 4.** Experimental data (symbols) and theory (lines) as a function of time for: a) Ion concentration in the solution reservoirs, i.e., diluate and concentrate, for the ED system with the newly-designed AEM; b-d) separation factor, $\beta_{NO_3^-/Cl^-}$, obtained with different AEMs. Duplicate symbols represent two independent sets of experiments.

(6 $cm^2$ of area available for ion transport) were separated by a silicone/polypropylene spacer (thickness 450 μm). Two cation exchange membranes (CEM, PC SC for ED 08002) were used to separate the electrode compartments from the cell pairs. Therefore, the stack has nine IEMs in total: 4 AEMs and 5 CEMs, of which the outer two CEMs are from the stack manufacturer (PC Cell). In the experiments with the newly-designed membranes, the CEMs used were Neosepta CMX. To test the performance of commercial IEMs, the ED stack was assembled with either the homogeneous membranes Neosepta AMX and CMX, or the heterogeneous membranes Ralex AMH-PES and CMH-PES.

The ED system was operated in batch-mode at a constant current density of $I = 20$ A/$m^2$. The fresh solution circulating through the diluate and concentrate compartments contains a binary salt mixture of $KNO_3$ (50 mM) and KCl (50 mM). Additionally, a $Na_2SO_4$ (0.1 M) solution was circulated between the electrode compartments. Throughout the experiments, samples from the diluate and concentrate reservoirs were taken every 30 min to measure ion concentration by ion chromatography.

The separation factor, $\beta_{a/b}$, at any time $t$ is obtained experimentally as

$$\beta_{a/b} = \frac{\Delta c_{a,c}}{\Delta c_{b,c}} \cdot \left(\frac{c_{b,d}}{c_{a,d}}\right)_t \tag{9}$$

where concentration differences $\Delta c_{i,c}$ refer to the change in reservoir concentration between the present and previous sample.

The flux of an ion across the membranes is calculated by

$$J_i = \frac{\Delta c_{i,j} \bullet V}{A \bullet \Delta t} \tag{10}$$

where $\Delta t$ is the time between two moments of sampling.

## 4. Results and discussion

### 4.1. Adsorption equilibrium experiments

The concentrations of $NO_3^-$ and $Cl^-$ in the AEMs were determined through adsorption experiments (Section 3.1). Fig. 3a shows that within the membranes, in theory, the total counterion concentration ($Cl^- + NO_3^-$) is approximately equal to the charge density, $X$, as reported in Table 1. The concentrations of co-ions in the membranes were very low and could not be detected by ion chromatography. These results show that highly charged IEMs—such as the membranes used in the present study—adsorb high concentrations of counterions that balance the functional groups in the membranes [12]. Interestingly, the three studied AEMs show higher adsorption of $NO_3^-$ over $Cl^-$ regardless of the

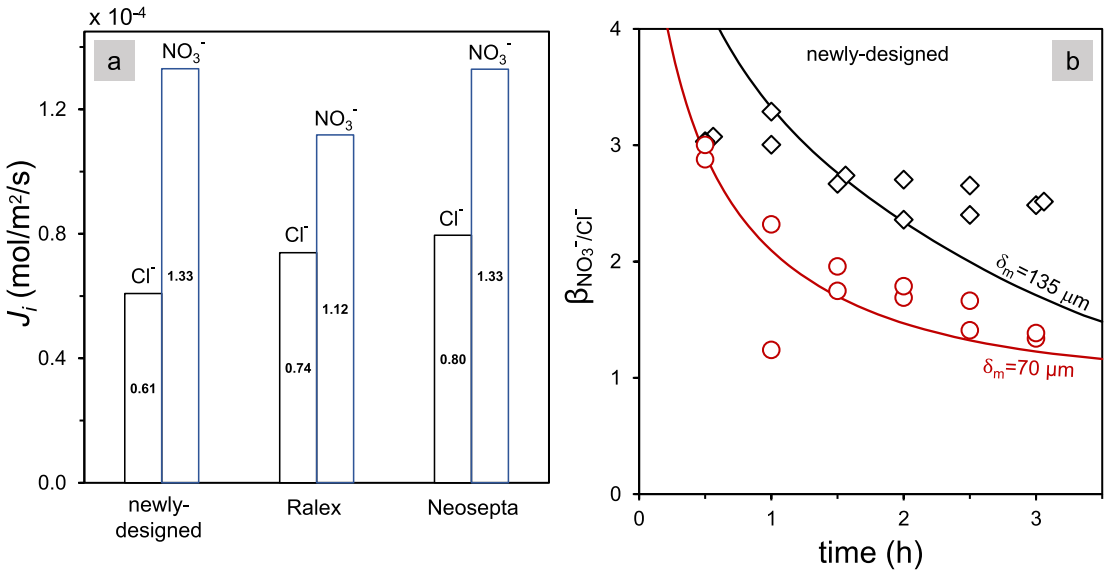


**Fig. 5.** a) Average flux of $NO_3^-$ and $Cl^-$ through AEMs calculated over a period of 3 h; b) separation factor, $\beta_{NO_3^-/Cl^-}$, for newly-designed AEMs with different membrane thickness, $\delta_m$, as function of time.

initial $NO_3^-$:$Cl^-$ concentration ratio, which translates into adsorption selectivities $S_{NO_3^-/Cl^-} > 1$ (Fig. 3b). However, the adsorption selectivity is markedly different between the membranes: the newly designed AEM is more selective for $NO_3^-$ than the commercial membranes.

We measured the adsorption of $NO_3^-$ and $Cl^-$ in AEMs to determine the value of the ion affinity, $\mu_i$, of $NO_3^-$ vs. $Cl^-$, which is introduced in the theory section as a parameter to quantify the preferential adsorption of ions in the IEMs. The affinity term is only calculated for $NO_3^-$, $\mu_{NO_3^-}$, and for other ions it is set to zero. In case of a high membrane charge density, *X*, the charge is predominantly compensated by counterions (such as anions in an AEM), and then only the differences between the μ-values are important, not the individual values.

We used the modified Boltzmann equation (see Eq. (5)) to calculate the ion concentration in the membranes. This equation describes the ion distribution at the membrane/solution interface and takes into account the contributions of ion charge, concentration, and ion affinity. The ion affinity $\mu_{NO_3^-}$ is derived by fitting theory to experimental data (the best-fit values are reported in Table 1). These values of $\mu_{NO_3^-}$ are introduced in our theory to describe the selective transport of ions across the membranes. Experimental and theoretical data of ion transport across the AEMs are presented in the next sections.

### 4.2. *Experiments and theory of ion transport in batch-mode ED*

In this section, we report experimental data and results of theoretical calculations of the competitive transport of $Cl^-$ and $NO_3^-$ through three different AEMs in ED. In batch-mode ED experiments, the concentrations of $Cl^-$ and $NO_3^-$ continuously decrease in the diluate reservoir and increase in the concentrate reservoir (Fig. 4a and Fig. S.I. 2). All three tested membranes transfer $NO_3^-$ faster than $Cl^-$. Fig. 4 also shows that theory (continuous lines), which includes the values of $\mu_{NO_3^-}$ that were obtained from the adsorption experiments (Fig. 3 and Fig. S.I. 1), closely describes measured ion concentrations. Theory shows a significant time-dependency of the selectivity, $\beta_{NO_3^-/Cl^-}$, of transport. However, experimentally, the changes of $\beta_{NO_3^-/Cl^-}$ are less pronounced and do not always show the same trends as the data. Comparing the newly-designed and Ralex membranes, we observe that despite similarities in their structure, mainly related to their heterogeneous nature [10,15], more $NO_3^-$ is transported through the newly-designed membrane, see Fig. 5a. On the other hand, the $NO_3^-$ flux through the newly-designed membrane is equal to that of the Neosepta membrane. However, the newly-designed membrane shows higher selectivity towards $NO_3^-$ because of the lower $Cl^-$ flux in comparison with Neosepta membranes.

In further theoretical studies with the newly-designed AEM, we found that $NO_3^-$ selectivity also depends on membrane thickness. Interestingly, results are that an increase in membrane thickness increases $\beta_{NO_3^-/Cl^-}$ (Fig. 5b). In the next section, we analyze how the transport of anions is affected by the membrane thickness and by other membrane parameters.

### 4.3. *Theoretical predictions of ion transport in continuous ED*

In this section, we present theoretical results of the transport of ions through a newly-designed AEM, i.e., the membrane with the highest $NO_3^-$ selectivity, in continuous ED, instead of batch-mode ED. In continuous ED, the system is in steady-state: the ion concentrations are not changing over time, which allows us to better understand and predict how the selective transport of $NO_3^-$ through IEMs is affected by membrane properties. Our study of preferential ion transport in continuous ED is also relevant because this operational mode is often used in large-scale ED desalination plants. In a continuous process, the aim is to achieve the desired concentration of the diluate stream with a single pass, depending on, amongst others, operational parameters such as the applied current and flow rate, and the dimensions of the system.

To analyze ion transport in continuous ED, we include certain modifications in the theory that was presented in Section 2. Consequently, the theory does not include a mass balance for the solution reservoirs (Eq. (8)), and hence $c_{i,j}$ in Eq. (6) does not change over time and is equal to the ion concentration in the feed solution. We consider an ED system in which the membranes have an active area of 100 $cm^2$, and the flow rate in each spacer channel is 1.5 mL/min. We systematically analyze the effect of parameters such as $\mu_{NO_3^-}$ and $D_m$ on the ion concentration profile in the membrane (S.I). We also study the effect of some membrane parameters, i.e., thickness and charge density, on $NO_3^-$ selectivity ($\beta_{NO_3^-/Cl^-}$).

### 4.4. *Effect of membrane parameters on ion selectivity*

We evaluated the effect of membrane thickness, $\delta_m$, charge density, *X*, and affinity $\mu_{NO_3^-}$ on the $NO_3^-$ selectivity of the newly-designed AEM

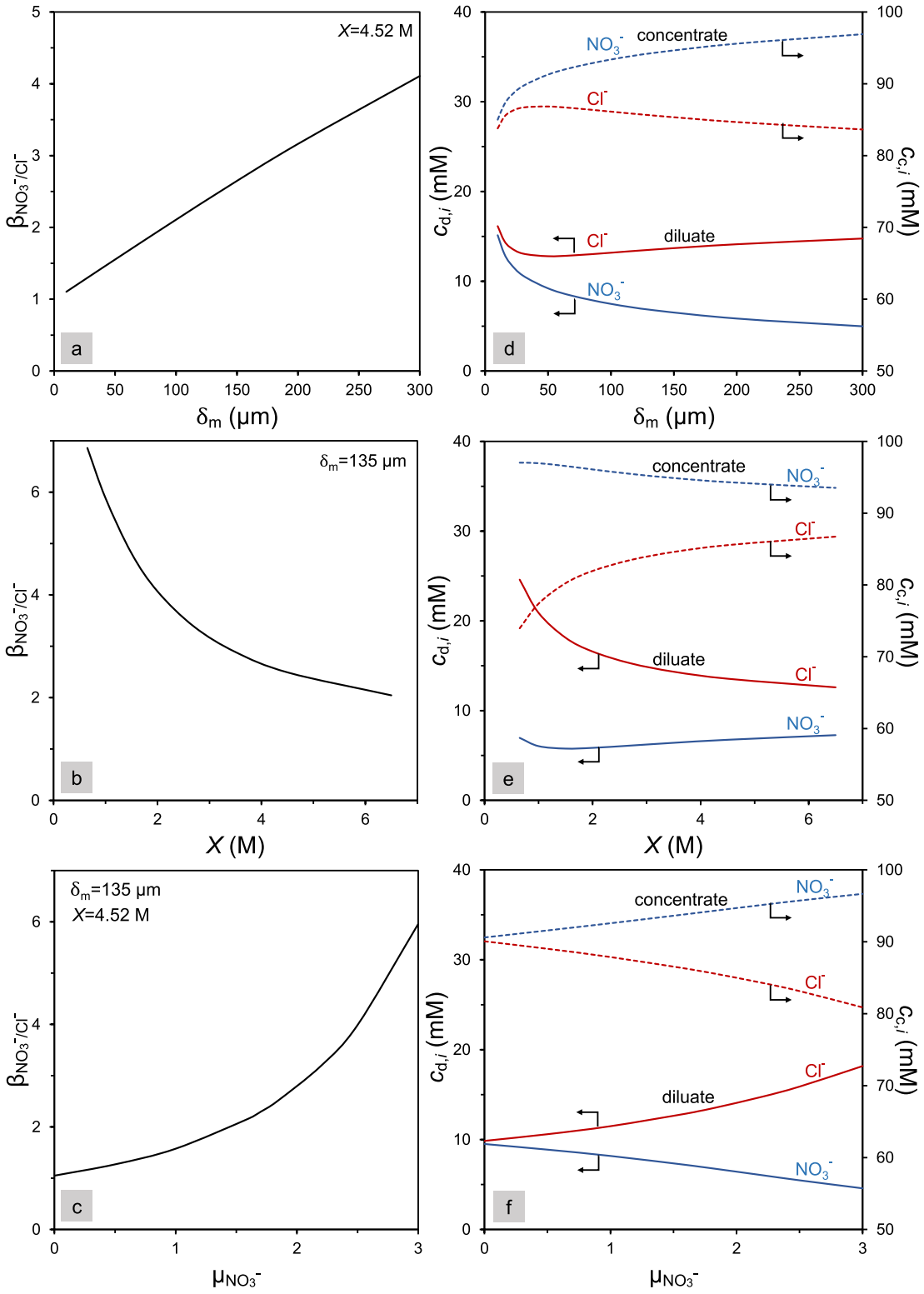


**Fig. 6.** Theoretical results for: a-c) Separation factor, $\beta_{NO_3^-/Cl^-}$, and d-f) concentration of anions in the spacer channels as a function of the membrane thickness, $\delta_m$, charge density, $X$, and the affinity term, $NO_3^-$.

(Fig. 6). Firstly, results in Fig. 6a show that increasing $\delta_m$ leads to an increase in the $NO_3^-$ concentration and a decrease in the $Cl^-$ concentration in the concentrate compartments. The opposite trend is observed in the diluate compartment (Fig. 6b). Increasing or decreasing $\delta_m$ has a pronounced effect on the anion concentration in the membrane at the membrane interface with the diluate channel (Fig. 7). However, at the interface with the concentrate channel, the $NO_3^-$ and $Cl^-$ concentrations are not significantly affected by $\delta_m$ (Fig. 7). To understand the relationship between $\delta_m$ and the ion concentration at the membrane interfaces in the membrane, we evaluate the transport of anions across the newly-designed AEM in terms of total flux and the contribution of diffusion, i.e., the flux of ions due to concentration gradients, and

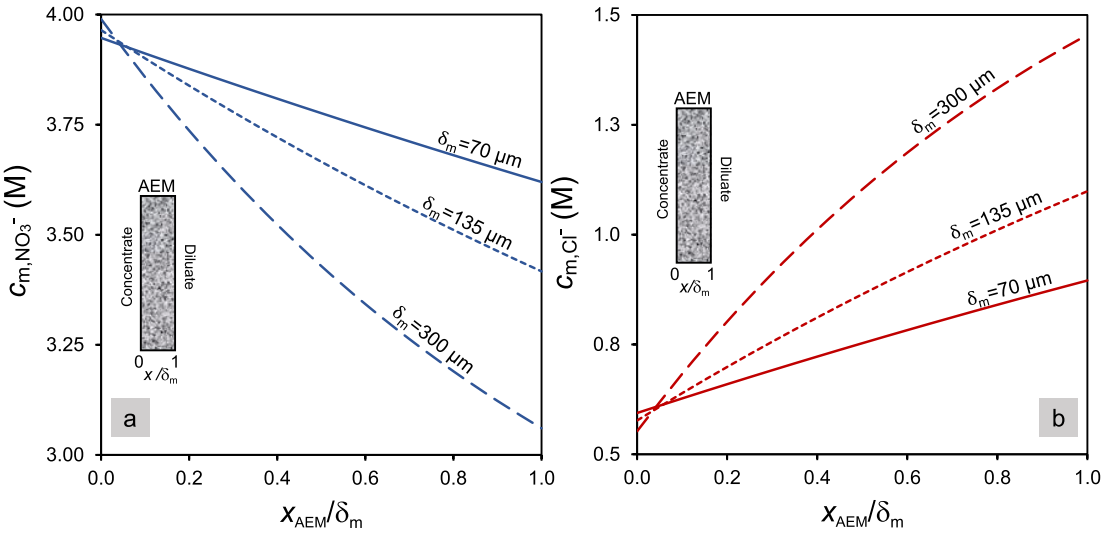


**Fig. 7.** Theoretical results for concentration profiles of a) $Cl^-$-ions and b) $NO_3^-$-ions assuming parameter settings based on the newly-designed membrane, for several values of the membrane thickness, $\delta_m$. The ratio $x_{AEM} / \delta_m$ is the position in the membrane, with $x_{AEM} / \delta_m = 0$ the concentrate-AEM interface, and $x_{AEM} / \delta_m = 1$ the AEM-diluate interface.

migration, i.e., the flux of ions due to the effect of electrical potential, (Fig. S.I. 4). For $NO_3^-$, the diffusion and migration fluxes at either interface do not markedly change with increasing $\delta_m$ (Fig. S.I. 4a–b). However,$\delta_m$ has a more dominant effect on the $Cl^-$ fluxes, especially at the membrane-diluate interface (Fig. S.I. 4c). Increasing $\delta_m$ causes a decrease in $Cl^-$ diffusion, while its migration flux increases across the membrane-diluate interface.

Secondly, Fig. 6c–d show the effect of $X$ on $\beta_{NO_3^-/Cl^-}$ and of the anion concentration in the spacer channels, when $\delta_m$ is kept constant (135 µm). Overall, increasing $X$ in the membrane decreases selectivity towards $NO_3^-$ (Fig. 6c). The change in $X$ has a more pronounced effect on the $Cl^-$ concentration than on the $NO_3^-$ concentration in the spacer channels (Fig. 6d). When we analyze the contribution of diffusion and migration to the total flux of $Cl^-$ (Fig. S.I. 5c–d), we observe that diffusion increases with increasing $X$, whereas migration decreases. Interestingly, for highly charged membranes (above 4.5 M) diffusion becomes the dominant contributor to $Cl^-$ transport. Thirdly, increased selectivity towards $NO_3^-$ is observed as $\mu_{NO_3^-}$ increases (Fig. 6e).

Overall, our results show that $NO_3^-$ selectivity can be enhanced when thick or low charge density AEMs are used. These results are in disagreement with the commonly accepted view of using membranes with reduced membrane thickness and increased charge density to optimize ED performance. This view is mainly based on the effect that the aforementioned membrane properties have on electrical resistance and selectivity towards counterions, which in turn affect the energy consumption of the ED system. However, selectivity between counterions is often not considered when analyzing membrane properties and their impact on ED operation. The effect of these membrane properties in systems with multiple salts was not investigated before, probably because of limitations on how to account for the affinity of the IEMs towards counterions, a topic we resolved in the present work.

## 5. Conclusions

We set up a theoretical model to describe the transport of mixtures of monovalent anions, i.e., $Cl^-$-ions and $NO_3^-$-ions, through various anion-exchange membranes (AEMs). In the model, we introduced an affinity term that describes the preferential adsorption of one ion over the other in a given membrane material. The affinity term combines all possible contributions (chemical and physical), except for a pure Donnan effect, that influence the interaction between counterions and the AEMs, and it therefore describes adsorption of a certain ion in the membrane in the presence of other ions. The transport model shows a reasonable agreement with data obtained in ED systems with three different types of AEMs operated in batch-mode.

Overall, with our model, it is possible to: i) explore strategies to modify the selectivity of ion-exchange membranes for a specific ion, ii) analyze the details of transport in AEMs where experimental data is difficult to obtain, for instance of ion concentration profiles in the membranes, and of the influence of parameters such as membrane charge density and thickness, and iii) analyze the contribution of different ion transport mechanisms, i.e., diffusion and migration.

With regard to ion selectivity in the AEMs, the data show that membrane properties such as thickness and charge density can be tuned to modify ion selectivity in a favored direction. Increasing the membrane thickness or decreasing its charge density are demonstrated to be possible strategies to increase the selectivity of $NO_3^-$ removal versus $Cl^-$ removal in AEMs.

## Declaration of Competing Interest

The authors declare that they have no known competing financial interests or personal relationships that could have appeared to influence the work reported in this paper.

## Acknowledgements

This work was performed in the cooperation framework of Wetsus, European Centre of Excellence for Sustainable Water Technology (www.wetsus.nl). Wetsus is co-funded by the Dutch Ministry of Economic Affairs and Ministry of Infrastructure and Environment, the European Union Regional Development Fund, the Province of Fryslân, and the Northern Netherlands Provinces. The author would like to thank the participants of the research theme “Capacitive Deionization" for the fruitful discussions and financial support.

## Appendix A. Supplementary material

Supplementary data to this article can be found online at https://doi.org/10.1016/j.seppur.2022.120944.

## References


[1] P.M. Biesheuvel, J.E. Dykstra, Physics of Electrochemical Processes (2020) ISBN: 9789090332581.

[2] P.M. Biesheuvel, S. Porada, M. Elimelech, J.E. Dykstra, Tutorial review of reverse osmosis and electrodialysis, J. Membr. Sci. 647 (2022) 120221, https://doi.org/10.1016/j.memsci.2021.120221.

[3] A. Campione, L. Gurreri, M. Ciofalo, G. Micale, A. Tamburini, A. Cipollina, Electrodialysis for water desalination: A critical assessment of recent developments on process fundamentals, models and applications, Desalination 434 (2018) 121–160.

[4] A. Chapotot, G. Pourcelly, C. Gavach, Transport competition between monovalent and divalent cations through cation-exchange membranes. Exchange isotherms and kinetic concepts, J. Membr. Sci. 96 (3) (1994) 167–181.

[5] A. Elattar, A. Elmidaoui, N. Pismenskaia, C. Gavach, G. Pourcelly, Comparison of transport properties of monovalent anions through anion-exchange membranes, J. Membr. Sci. 143 (1-2) (1998) 249–261.

[6] R. Epsztein, E. Shaulsky, M. Qin, M. Elimelech, Activation behavior for ion permeation in ion-exchange membranes: Role of ion dehydration in selective transport, J. Membr. Sci. 580 (2019) 316–326.

[7] A.H. Galama, G. Daubaras, O.S. Burheim, H.H.M. Rijnaarts, J.W. Post, Seawater electrodialysis with preferential removal of divalent ions, J. Membr. Sci. 452 (2014) 219–228.

[8] A.H. Galama, J.W. Post, M.A. Cohen Stuart, P.M. Biesheuvel, Validity of the Boltzmann equation to describe Donnan equilibrium at the membrane–solution interface, J. Membr. Sci. 442 (2013) 131–139.

[9] A.G. Guzmán-Garcia, P.N. Pintauro, M.W. Verbrugge, R.F. Hill, Development of a Space-Charge Transport Model for Ion-Exchange Membranes, AIChE J. 36 (7) (1990) 1061–1074.

[10] S.M. Hosseini, A. Gholami, S.S. Madaeni, A.R. Moghadassi, A.R. Hamidi, Fabrication of (polyvinyl chloride/cellulose acetate) electrodialysis heterogeneous cation exchange membrane: Characterization and performance in desalination process, Desalination 306 (2012) 51–59.

[11] N. Kabay, Ö. İpek, H. Kahveci, M. Yüksel, Effect of salt combination on separation of monovalent and divalent salts by electrodialysis, Desalination 198 (1-3) (2006) 84–91.

[12] J. Kamcev, D.R. Paul, B.D. Freeman, Effect of fixed charge group concentration on equilibrium ion sorption in ion exchange membranes, J. Mater. Chem. A 5 (9) (2017) 4638–4650.

[13] Y. Kim, W.S. Walker, D.F. Lawler, Competitive separation of di- vs. mono-valent cations in electrodialysis: effects of the boundary layer properties, Water Res 46 (7) (2012) 2042–2056.

[14] T. Luo, S. Abdu, M. Wessling, Selectivity of ion exchange membranes: A review, J. Membr. Sci. 555 (2018) 429–454.

[15] T. Mubita, S. Porada, P. Aerts, A. van der Wal, Heterogeneous anion exchange membranes with nitrate selectivity and low electrical resistance, J. Membr. Sci. 607 (2020) 118000, https://doi.org/10.1016/j.memsci.2020.118000.

[16] A. Münchinger, K.-D. Kreuer, Selective ion transport through hydrated cation and anion exchange membranes I. The effect of specific interactions, J. Membr. Sci. 592 (2019) 117372, https://doi.org/10.1016/j.memsci.2019.117372.

[17] R.K. Nagarale, G.S. Gohil, V.K. Shahi, Recent developments on ion-exchange membranes and electro-membrane processes, Adv. Colloid Interface Sci. 119 (2-3) (2006) 97–130.

[18] V. Nikonenko, V. Zabolotsky, C. Larchet, B. Auclair, G. Pourcelly, Mathematical description of ion transport in membrane systems, Desalination 147 (1-3) (2002) 369–374.

[19] J.M. Ortiz, J.A. Sotoca, E. Expósito, F. Gallud, V. García-García, V. Montiel, A. Aldaz, Brackish water desalination by electrodialysis: batch recirculation operation modeling, J. Membr. Sci. 252 (1-2) (2005) 65–75.

[20] P.N. Pintauro, D.N. Bennion, Mass Transport of Electrolytes in Membranes. 1. Development of Mathematical Transport Model, Ind. Eng. Chem. Fundam. 23 (2) (1984) 230–234.

[21] P.N. Pintauro, D.N. Bennion, Mass Transport of Electrolytes in Membranes. 2. Determination of NaCI Equilibrium and Transport Parameters for Nafion, Ind. Eng. Chem. Fundam. 23 (1984) 234–243.

[22] S. Porada, L. Zhang, J.E. Dykstra, Energy consumption in membrane capacitive deionization and comparison with reverse osmosis, Desalination 488 (2020) 114383, https://doi.org/10.1016/j.desal.2020.114383.

[23] E. Quenneville, M. Buschmann, A transport model of electrolyte convection through a charged membrane predicts generation of net charge at membrane/electrolyte interfaces, J. Membr. Sci. 265 (1-2) (2005) 60–73.

[24] L.A. Richards, A.I. Schäfer, B.S. Richards, B. Corry, The Importance of Dehydration in Determining Ion Transport in Narrow Pores, Small 8 (11) (2012) 1701–1709.

[25] M. Sadrzadeh, A. Razmi, T. Mohammadi, Separation of different ions from wastewater at various operating conditions using electrodialysis, Sep. Purif. Technol. 54 (2) (2007) 147–156.

[26] T. Sata, Studies on anion exchange membranes having permselectivity for specific anions in electrodialysis — effect of hydrophilicity of anion exchange membranes on permselectivity of anions, J. Membr. Sci. 167 (1) (2000) 1–31.

[27] T. Sata, T. Yamaguchi, K. Matsusaki, Effect of Hydrophobicity of Ion Exchange Groups of Anion Exchange Membranes on Permselectivity between Two Anions, J. Phys. Chem. 99 (34) (1995) 12875–12882.

[28] K. Tado, F. Sakai, Y. Sano, A. Nakayama, An analysis on ion transport process in electrodialysis desalination, Desalination 378 (2016) 60–66.

[29] M. Tedesco, H.V.M. Hamelers, P.M. Biesheuvel, Nernst-Planck transport theory for (reverse) electrodialysis: I. Effect of co-ion transport through the membranes, J. Membr. Sci. 510 (2016) 370–381.

[30] X. Xu, Q. He, G. Ma, H. Wang, N. Nirmalakhandan, P. Xu, Selective separation of mono- and di-valent cations in electrodialysis during brackish water desalination: Bench and pilot-scale studies, Desalination 428 (2018) 146–160.

[31] Y. Yang, P.N. Pintauro, Multicomponent Space-Charge Transport Model for Ion-Exchange Membranes, AIChE J. 46 (6) (2000) 1177–1190.

[32] V.I. Zabolotsky, J.A. Manzanares, V.V. Nikonenko, K.A. Lebedev, E.G. Lovtsov, Space charge effect on competitive ion transport through ion-exchange membranes, Desalination 147 (1-3) (2002) 387–392.

[33] R. Zhao, O. Satpradit, H.H.M. Rijnaarts, P.M. Biesheuvel, A. van der Wal, Optimization of salt adsorption rate in membrane capacitive deionization, Water Res. 47 (5) (2013) 1941–1952.

[34] A.N. Shocron, E.N. Guyes, P.M. Biesheuvel, H.H.M. Rijnaarts, M.E. Suss, J. E. Dykstra, Electrochemical removal of amphoteric ions, Proceedings of the National Academy of Sciences 118 (2021) e2108240118.